

Aalto University, School of Science and Technology
Faculty of Engineering and Architecture.
Department of Applied Mechanics. Series AM
eknillinen korkeakoulueknillinen korkeakoulu. Insinööritieteiden ja arkkitehtuurin tiedekunta.
Sovelletun mekaniikan laitos. Sarja AM
Espoo 2010, FINLAND

TKK-AM-15

Investigation on employing ships as sensors for ice thickness measurements

R.U.F. von Bock und Polach



Table of Contents

Symbols.....	3
Abstract.....	4
Introduction.....	4
1. The Cruise.....	5
2. Measurements.....	5
2.1. Systematic Error Analysis.....	5
2.2. Temperature Measurements.....	6
2.3. Salinity profile.....	7
2.4. Bending strength measurements.....	7
2.4.1. Background.....	7
2.4.2. Measurement Device.....	8
2.4.3. Results.....	8
2.5. Crushing Strength Measurements.....	11
2.5.1. Procedure.....	11
2.5.2. Vertical Crushing Strength.....	13
2.5.3. Horizontal Crushing Strength.....	14
3. Ship Properties.....	16
3.1. General Dimensions.....	16
3.2. Ship status and condition.....	16
3.3. Engines, Generators and propulsion system.....	16
3.3.1. Propeller properties.....	16
3.3.2. Propulsion System.....	17
3.3.3. Engine power and shaft power.....	18
3.4. Engines and Generators.....	18
3.4.1. Main engine # 1.....	18
3.4.2. Main engine # 2.....	21
3.5. Propeller shaft power.....	21
4. Cruise data and map.....	23
5. Open Water Performance.....	24
6. Performance in ice.....	25
6.1. Theoretical performance in ice.....	25
6.2. Practical performance in ice.....	28
6.2.1. Measurements.....	28
6.2.2. Evaluation of the measurements.....	31
6.3. Accuracy of the assessment of the performance in ice.....	31
7. Summary.....	32
8. Conclusions.....	32
References.....	32

Symbols

A_{WF}	Waterline area of the foreship
B	Beam
BOB	Bay Of Bothnia – Abbreviation for ice stations
D_P	Propeller Diameter
F_n	Froude Number
K_0	Coefficient of lateral stress at rest
H_F	Thickness of brash ice layer
H_M	Channel thickness
K_e	Propeller Efficiency
K_p	Coefficient of passive stress
L_{bow}	Length of bow portion of ship at waterline
L_{par}	Length of parallel midbody section of the ship at the waterline
L_{pp}	Length between perpendiculars
P_S	Shaft Power
R_{ch}	Channel resistance
R_i	Ice resistance
T	Draft
T_{net}	Net Thrust
T_{pull}	Bollard Pull Thrust
a	Waterplane entrance angle
d	The angle of the side wall of the brash ice
f	Angle between the waterline and the vertical at $B/2$
g	Gravity
h_i	Ice thickness
m_B	1-p
m_h	Hull/ice friction
r_Δ	Difference between densities of water and ice
v	Velocity
v_{ow}	Open Water Velocity
z	System function for systematic error
α	Flare angle
Δz	Systematic error

Abstract

The project *Investigation on employing ships as sensors for ice thickness measurements* has been carried out for the Ship Sensor Net (SSN) project. The SSN project was founded by the TEKES Ubicom program. The contribution of this report to the SSN project was to investigate whether it was possible to employ ships as sensors to measure the ice thickness. According to hull shape, engine and machinery setting every ship has her signature for sailing in ice, which is expressed by curves of level ice thickness over ship speed curves (h-v curve). The h-v curve allows determining the encountered level ice thickness from ship speed.

In order to test the h-v curve a research cruise was conducted aboard RV Aranda. During the cruise in ice also other properties than the ice thickness have been measured in order to assess in how far a variation of those might affect the ship's performance. The determining of the ice thickness with Aranda as a sensor delivered very scattered results and from the measurement of the ice properties it could be seen that the ice properties were also subjected to a lot of scatter, which leaves it still open whether the approach of employing a ship as an ice thickness measurement sensor was successful or not.

Introduction

The scope of the ShipSensorNet project was to establish a system that uses ships travelling through ice as a sensor in order to determine the ice properties by monitoring the ship speed.

In March 2009 an ice cruise was ventured with the research vessel Aranda owned by FMI, with the purpose to elaborate the opportunities of using the ships as a sensor to assess the ice thickness. During the cruise three ice camps were established in order to measure the sea ice properties such as bending strength, crushing strength, ice temperature and salinity. During the transit in level ice, the ice thickness was estimated visually and the speed of the ship was recorded simultaneously in order to determine an empirical h-v curve (ice thickness vs. ship speed curve). The target is to elaborate whether it is possible to determine the ice thickness just by monitoring the speed of a ship.

Since it did not succeed in the beginning to save the monitored data of the APIS engine control system and to synchronize them with the ship's on board system, it was not possible to collect data throughout the whole voyage.

1. The Cruise

The cruise was carried out with the Aranda, the research vessel of the FMIR. The cruise leads to the following locations where samples for measurements have been taken.

Table 1: Locations of ice stations

Location Name	Coordinates	Longitude / Latitude
BOB 1	64deg 00.587'	North
	21deg 19.995'	East
BOB 2	64deg 00.360'	North
	21deg 18.628'	East
BOB 3	64deg 20.778'	North
	22deg 13.805'	East

In the area of BOB2 the ship was trapped in ice drift and thus the location was soon abandoned and only a few measurements have been conducted.

2. Measurements

2.1. Systematic Error Analysis

The measurements are subjected to inaccuracies related to the used devices and the consecutive systematic error in the measurements. That means that any inaccuracy in any measured parameter is affecting the overall accuracy of the measurements. The systematic error is determined by the following equation.

$$\Delta z \approx \sum_{i=1}^n \frac{\partial z}{\partial x_i} \Delta x_i \quad (1)$$

In equation (1) the systematic error Δz is determined in dependence on the influencing parameters. The parameter z is the equation that contains all parameters needed to determine the parameter of interest. In case of the crushing strength of ice the function Δz looks as follows.

$$z = \frac{\text{Force}}{\text{width} \times \text{length}} = \frac{F}{a \cdot b} \quad (2)$$

For the systematic error Δz the function z must be differentiated by all containing parameters F, a, b and is then multiplied by the accuracy, offset or error of the particular parameter. In case of the ice block dimensions that would be 0.5 mm which is the accuracy with what the dimensions can be determined / measured.

The analysis of the accuracy is again based on the theory of the systematic error analysis. The error depends on the influencing parameters and thus on the specimen type which means it matters whether it was a core or a cut brick, since different parameters need to be taken into account. The weight-scaling accuracy is included as well since the plate that is distributing the load over the surface of the ice sample affects the result and must be added to the downward force crushing the ice block.

Since it was difficult to obtain very accurate straight bricks the uncertainty of the straightness was included in the accuracy of the dimension measurements. Parameters affecting the accuracy of a rectangular brick are:

- Width (accuracy 1.5mm)
- Height (accuracy 1.5mm)
- Load-cell (accuracy 0.5%)
- Scale accuracy (5g)

Parameters affecting the accuracy of a cylindrical core are:

- Diameter (accuracy 1mm)
- Load-cell (accuracy 0.5%)
- Scale accuracy (5g)

2.2. Temperature Measurements

The mechanical properties of the ice are affected by the temperature gradient over the ice thickness. The temperature in the ice depends on the sea water temperature at the bottom of the ice, the ambient air temperature on top of the ice and the heat capacity of the ice.

The temperatures in the ice have been taken right after the ice block has been taken out of the water and before the strength measurements have been carried out. All temperature measurements that have been taken in one location have been averaged and compiled in Figure 1 which shows that the ice temperature at location BOB 3 is significantly lower than at BOB 1 which can be one explanation for the different mechanical properties (Figure 14) in both locations.

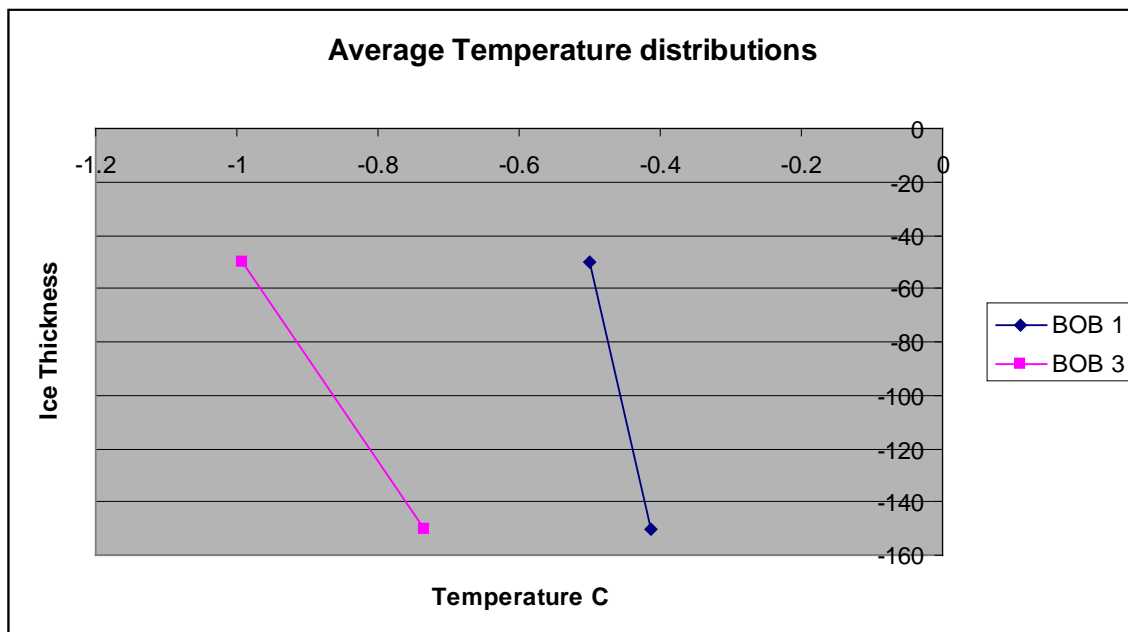


Figure 1: Temperature distribution in ice

2.3. Salinity profile

The salinity of the ice is affecting the mechanical properties of the ice and the higher the salinity the more the strength decreases. The salinity is measured in ppt (parts per thousand). The average salinity of all measured samples was location independent and resulted in a salinity concentration of 0.55 ppt.

At the locations BOB1 and BOB3 the ice samples have been cut in segments in order to make a salinity profile. The nature of the salinity distribution at BOB 1 as expected, unlike the salinity distribution at BOB 3. At location BOB 3 several salinity measurements have been carried out in order to check the extraordinary salinity distribution that is reflected by the average values in Figure 2, but all measured results confirmed the same salinity distribution.

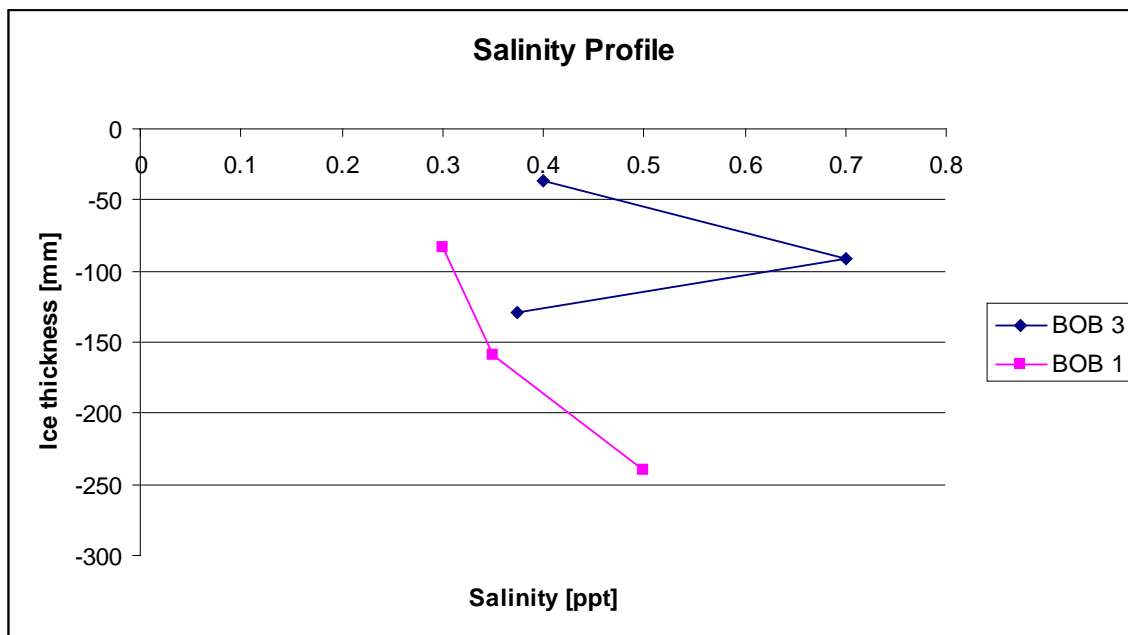


Figure 2: Salinity Profile

2.4. Bending strength measurements

2.4.1. Background

Bending strength measurements are rarely subjected to full scale measurements, because in-situ measurements with a cantilever beam are difficult to be carried out.

The ice properties such as the bending strength can have a significant impact on the ice resistance and the advancing speed of the ship and thus it was decided to try to measure the bending strength with a different approach.

The idea is to support an ice beam (dimensions according to ITTC [2]) on two pipes and loaded by the hydraulic press, whereas the load is applied by another pipe in order to avoid unwanted stress concentrations. The load that is measured as ultimate load is used to determine the flexural strength by applying basic mechanical models. Most of the

tested ice beams have been of the dimensions 330mm x 90mm x 40 mm (Length x Width x Height)

It must be clarified that the measured and calculated strength is probably not the real bending strength of the ice.

Natural grown ice can have grain diameters between 1mm and 20mm Cammaert et al. [7] (in some cases up to 1m diameter) and therefore the used sampled are relatively small and have consequently less grain boundaries. Grain boundaries are sources of defects, preferential sites for impurities and serve as sites for crack nucleation, Schulson and Duval [6]. If a test specimen is relatively small, a scale effect is encountered and the measured bending strength is higher than the one encountered by a ship. Since however the specimen size and bending strength testing procedure are the same for all tests, the bending strength variation is considered being representative even if the absolute value is not.

2.4.2. Measurement Device

The hydraulic press was equipped with a stamp made of a plastic pipe. The pipe made sure that no sharp edges were pressed into the ice causing stress concentrations. The same is valid for the supports which were made of round steel pipes. The device can be seen in Figure 3.



Figure 3: Bending strength measurements

2.4.3. Results

The idea for setting up a device to measure the bending strength as seen in Figure 3 came up during the transit from BOB 1 to BOB 2 and thus no bending strength values are available from BOB 1.

Figure 4 and Figure 5 show the average bending strength distribution over the thickness. The strength distribution in the upper 2 levels is almost similar in the two locations, but it deviates for the lower layer. The phenomenon was also cross-checked by salinity measurements and it was found that at BOB 3 the salinity in the bottom layer was the highest unlike at BOB 2.

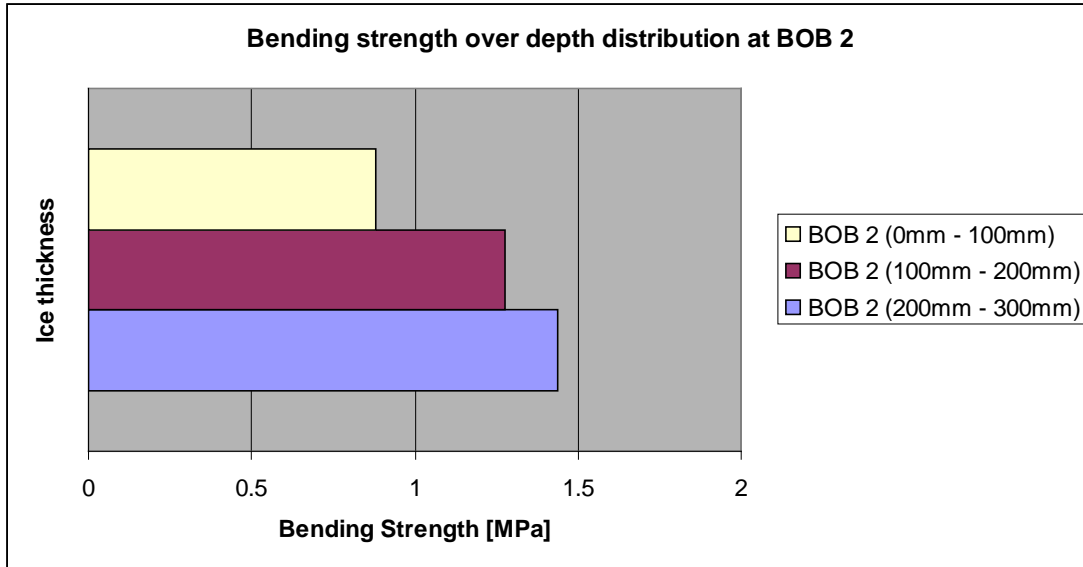


Figure 4: Average bending strength distribution at BOB 2

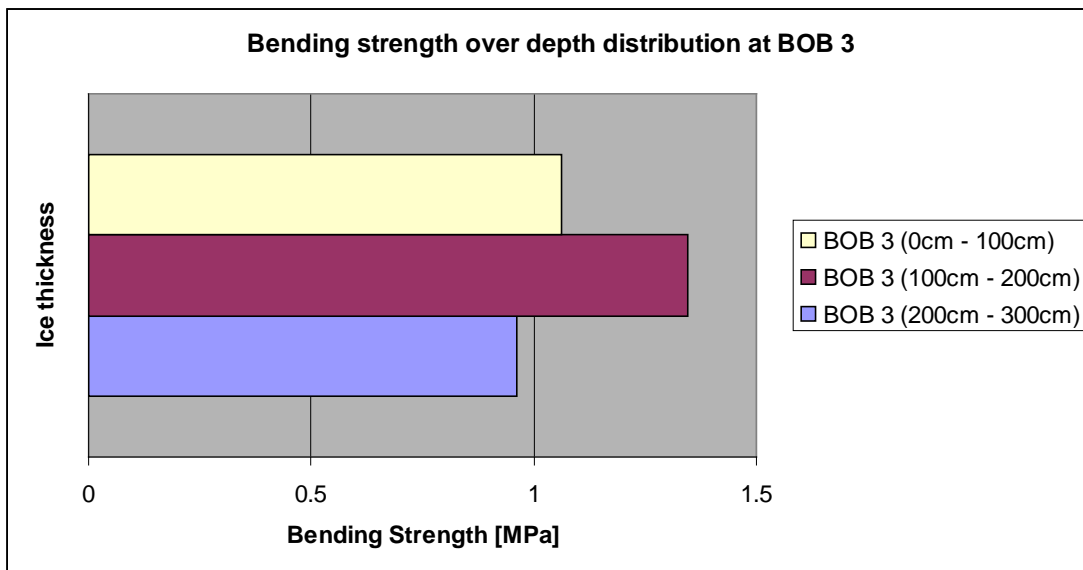


Figure 5: Average bending strength distribution at BOB 3

Figure 6 shows that the average bending strength per taken ice sample is subjected to some variation, but variations appear to be within the same limits in both locations.

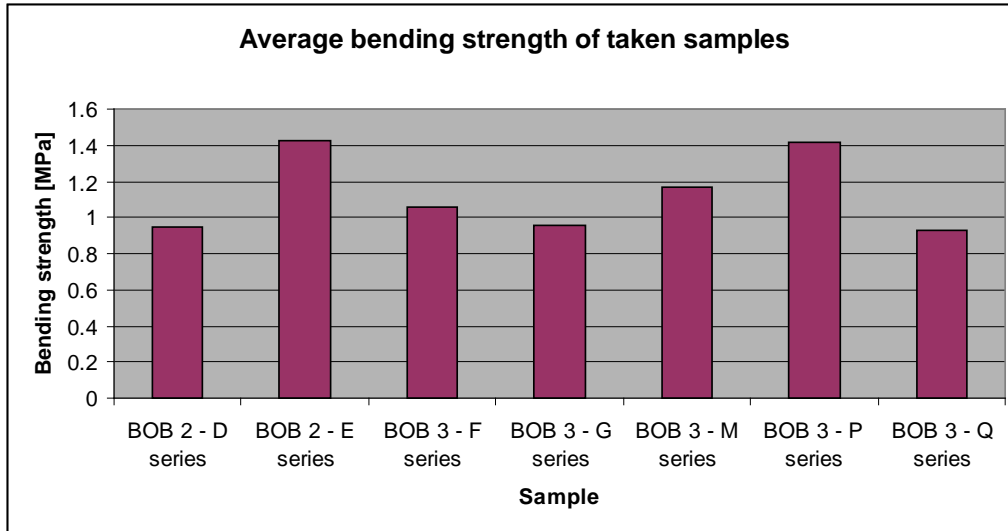


Figure 6: Average bending strength of the taken samples

Figure 7 and Figure 8 reflect the measured bending strength values including the uncertainty range of the systematic error. Both locations are subjected to similar trends in terms of bending strength.

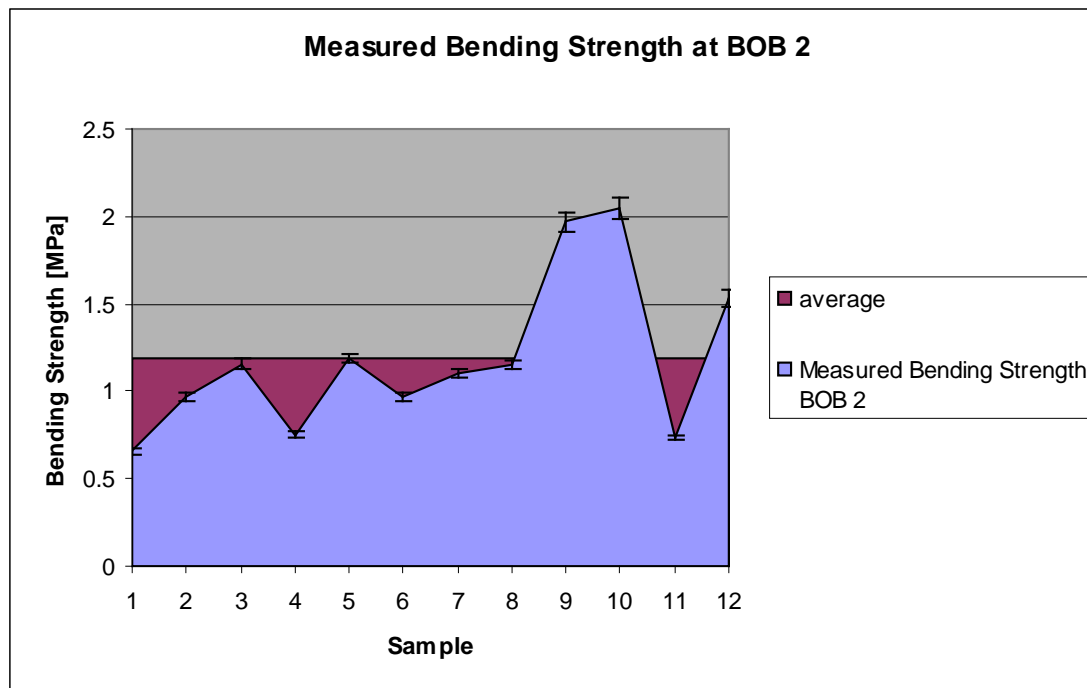


Figure 7: Average and absolute bending strength at BOB 2

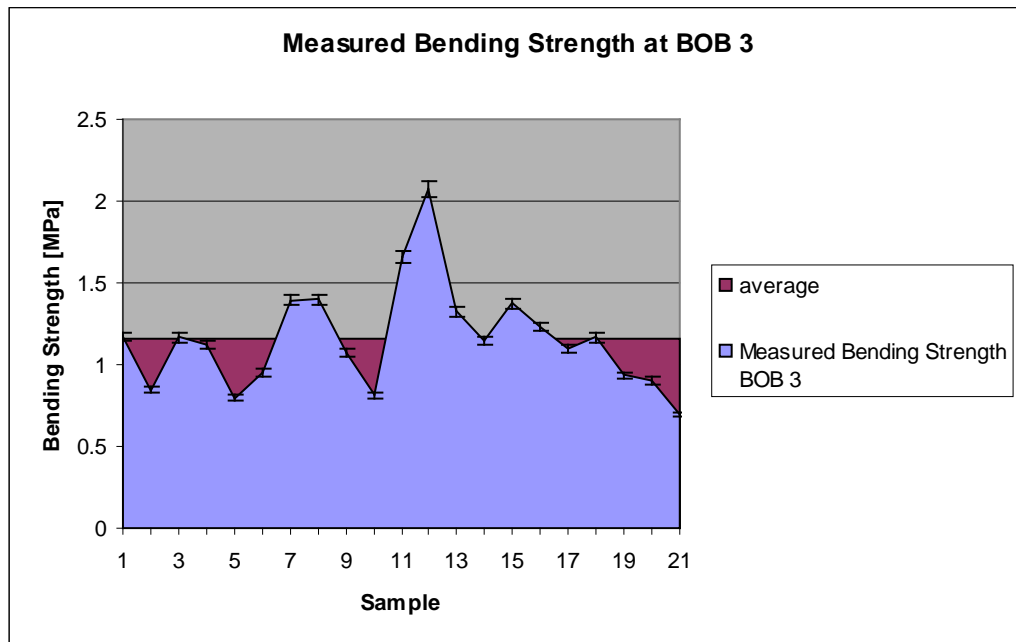


Figure 8: Average and absolute bending strength at BOB 3

Kujala [4] carried out flexural strength measurements and obtained values of around 0.9 MPa, whereas Enqvist [4] obtained average values around 0.5 MPa. In [4] it is stated that the test method and scale effects (Section 2.4.1) might affect the results. The measurements stated in this report have been carried out with a new method, which might have led to the relatively high average values of around 1.2 MPa. Although the absolute values differ from previous measurements, the test procedure has always been exactly the same and thus it is believed that there was a clear variation in the ice properties depending on the location.

2.5. Crushing Strength Measurements

2.5.1. Procedure

The vertical crushing strength was determined from samples shaped as rectangular blocks and cylindrical ice cores. In contrast to the horizontal crushing strength the vertical crushing strength is not depending on its position within the ice block, since the sample was more or less taken over the entire height. Top and bottom of the original sample were cut off in order to provide a smooth plain surface.

The ice cores were cut into several layers in order to fit them into the hydraulic press seen in Figure 9. The measurements have been performed immediately after the ice samples were cut out of the ice. The height of the samples had to be between 10cm and 15cm. Since ice is a non isotropic material the crushing strength has been assessed for samples that were orientated horizontal and vertical.

For both the vertical and the horizontal crushing strength the tests have been carried out following the same procedure.

The steps of the procedure were as follows:

1. Cutting out an ice block in-situ
2. Carrying the ice block immediately on board
3. Cutting the ice block into pieces according to the right dimension

Since ice is a very non-homogeneous material and non-isotropic material, many more measurements would be required in order to generate a representative profile of the strength distribution. Since the tests have always been carried out following the same procedure the tests represent the variations of the ice very well.



Figure 9: Ice crushing



Figure 10: Crushed ice sample

2.5.2. Vertical Crushing Strength

Vertical crushing strength means that the sample was taken vertically out of the ice-block i.e. that the top and the bottom are taken from different height-levels of the ice.

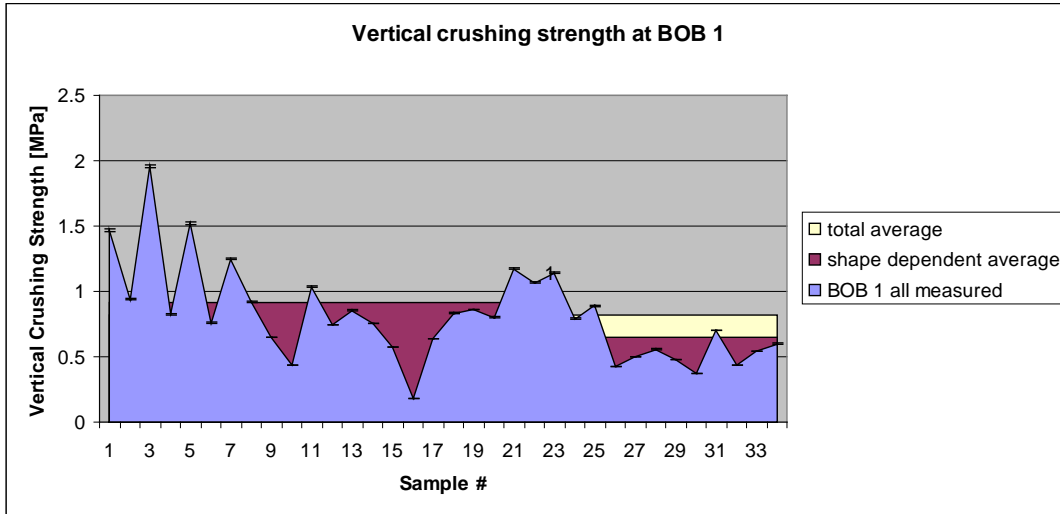


Figure 11 Shape influence on strength values

From sample 1 to 21 the crushing strength has been measured with ice bricks and the rest was determined by ice cores for the results from the location BOB 1. According to Figure 11, the cylindrical cores reflect a much lower crushing strength than the cut bricks. In the very beginning it was realized that the crushing strength respectively the ice samples react very sensitive on heat. In the very beginning the measurement series has been carried out with ice samples that have been stored on deck and were for 30min subjected to the sun and the measured crushing strength was very low. For the ice cores a similar effect might occur since the long drilling process might induce a significant amount of heat. It is still possible that this phenomenon is subjected to other reasons; however this reason is believed to be the most likely.

A comparison of Figure 11, Figure 13 and Figure 12 shows a significant difference between the strength values of the different locations.

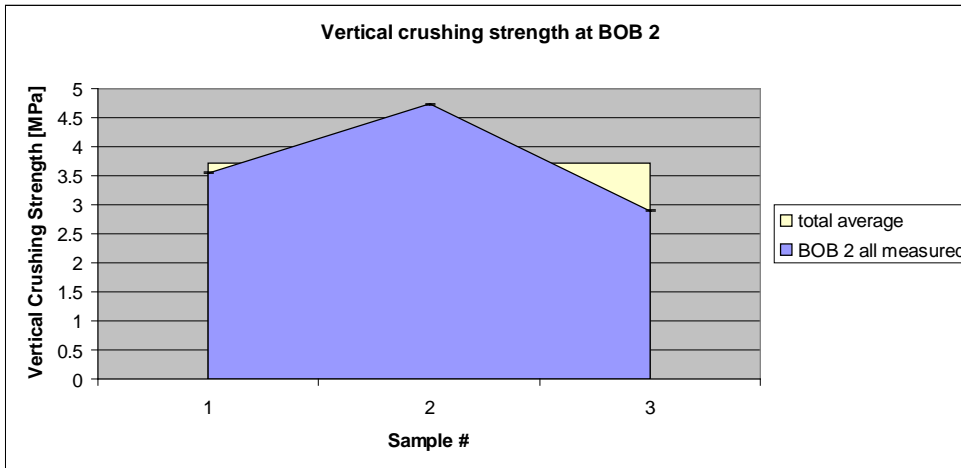


Figure 12: Vertical crushing strength at BOB2

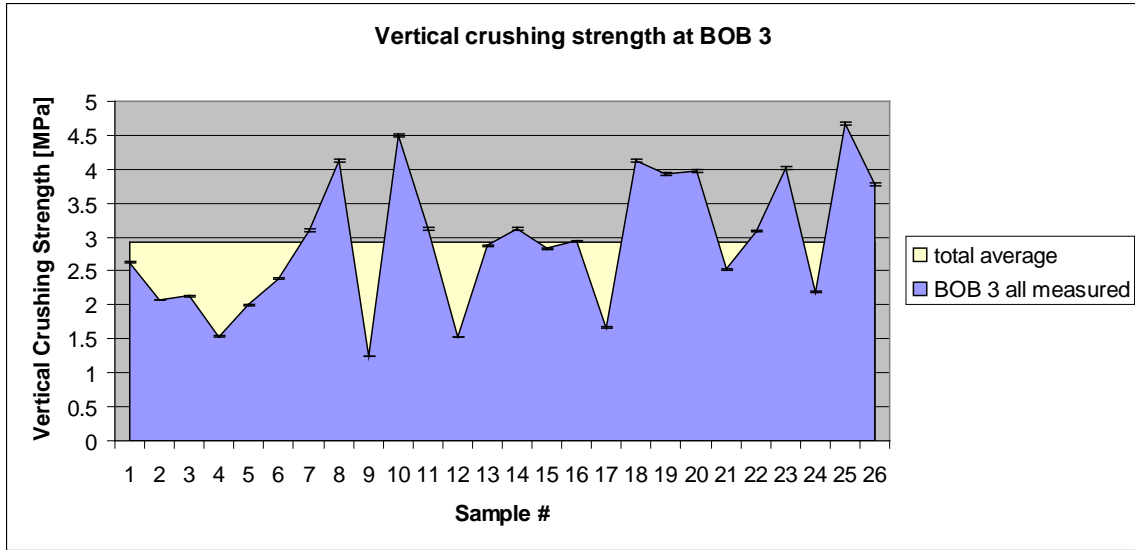


Figure 13: Vertical Crushing Strength at BOB3

2.5.3. Horizontal Crushing Strength

The ice block was cut into several slices over the depth in order to appraise the variation of the strength in dependence of the position in the ice thickness. Unlike the vertical crushing strength, the surfaces on which the loads are applied are taken from the same thickness-level.

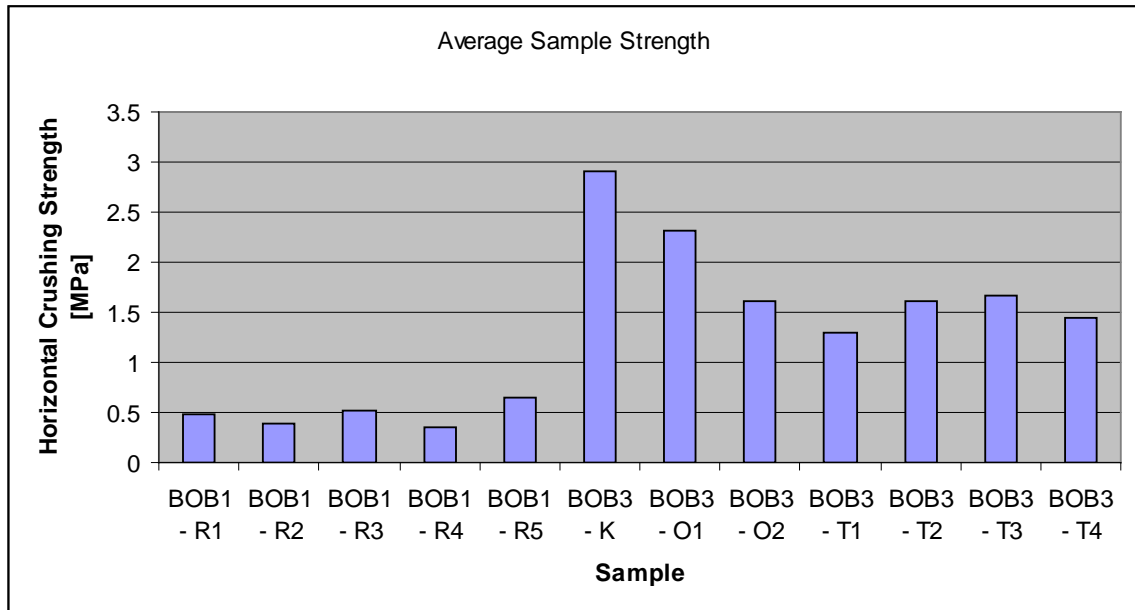


Figure 14: Average horizontal crushing strength of all taken samples

Figure 14 shows the average horizontal crushing strength of the taken ice samples at the locations BOB1 and BOB3. The obtained strength values point out that there is a differences between the samples of each location. The difference between the values obtained from location BOB1 and BOB3 are much higher which might be subjected to

various reasons such as ice formation history and ice temperature, which can not be evaluated here. However the difference in temperature (Figure 1) gives good evidence that the obtained differences in strength are valid.

In Figure 15 and Figure 16 the absolute value of each measurement value is reflected including the possible maximum and minimum value according to the systematic error analysis. The low maximum error of 0.5% was mainly related to the fact that only a few parameters influenced the measurements. The figures represent well the variation from sample to sample, but also the big difference in the ice properties depending on the locations BOB 1 and BOB 3.

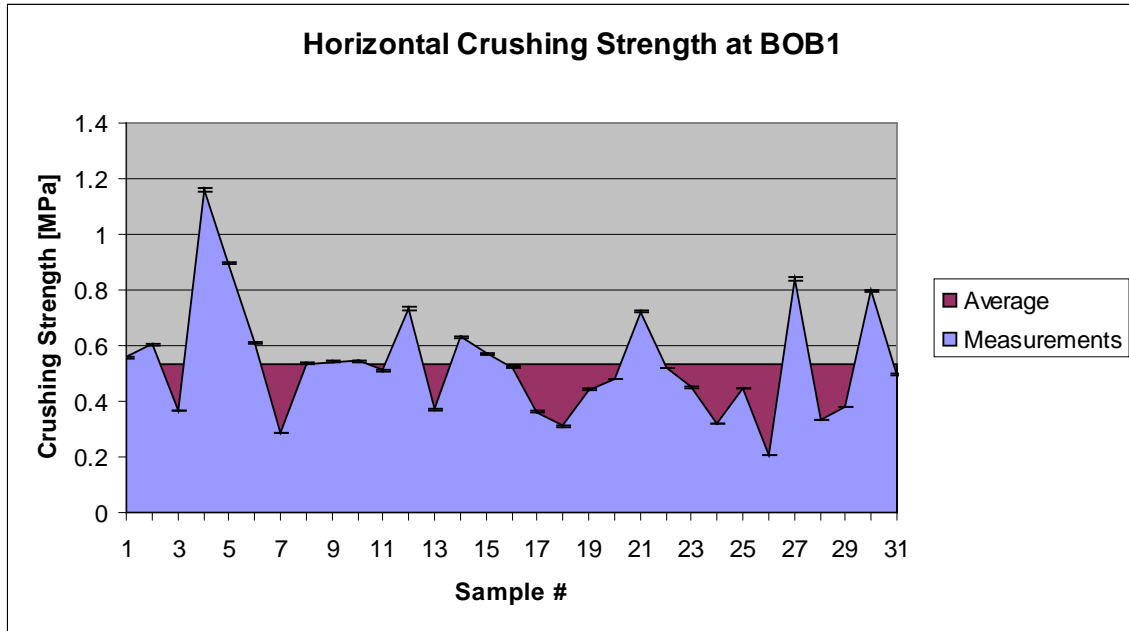


Figure 15: Horizontal Crushing Strength at BOB 1

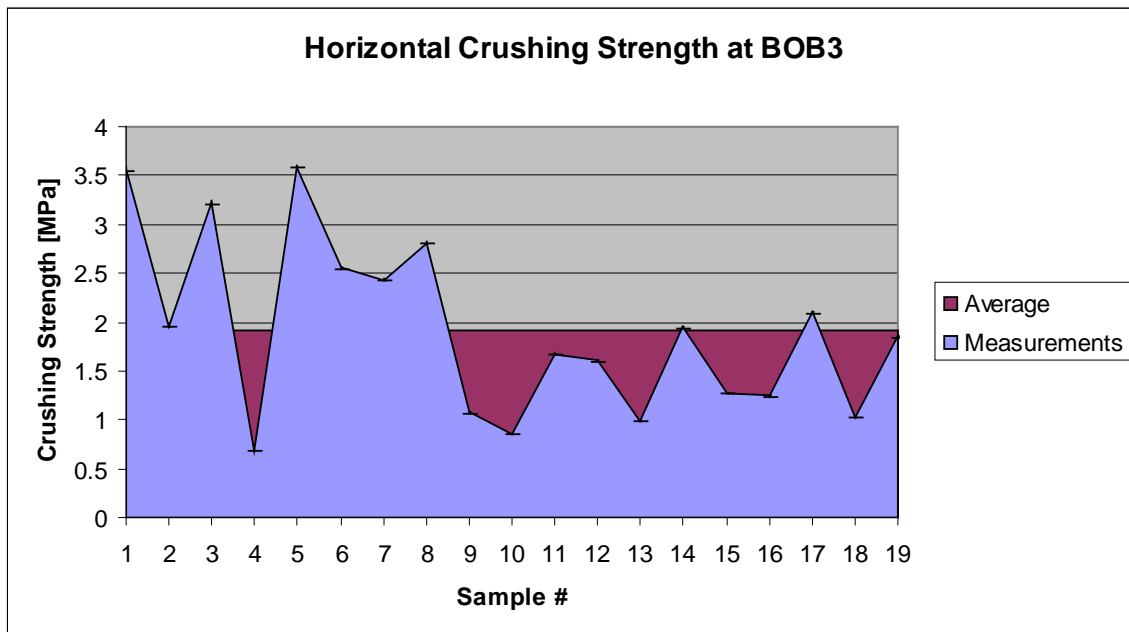


Figure 16: Horizontal Crushing Strength at BOB 3

According to Kujala [4] the horizontal crushing strength of previous tests lies between 1.4 MPa – 4.5MPa (Varsta 1983) and 1.25 MPa – 3.3 MPa (Fransson and Elfgrén 1987). According to the measurements seen in Figure 15 and Figure 16 the measured values during the research cruise lie within the limits of previous measurements.

3. Ship Properties

3.1. General Dimensions

The ship is a research vessel and run by the Finnish Maritime Institute. The general dimensions are:

LOA: 59.24m
Lpp: 52.20m
Bmax: 13.80m
Design draft: 4.6m
Dmax: 5m
Stem angle 31deg
Waterline ang 36deg.

The waterline angle for the draught of 4.6m was determined from the waterline angle on the decks at 6.7m and 4.2m for frame 85 at the tip of the bow. The interpolation has been done linear due to simplicity and since only two vertices were available from the general drawings.

3.2. Ship status and condition

Table 2 reflects the changes in the loading condition over the time and since these changes are small it is considered that those changes are not affecting the performance in ice and can not be related to any variations in resistance.

Table 2: Loading condition of Aranda

	02.03.2009	07.03.2009	09.03.2009	11.03.2009
Mean draft	4.59 m	4.53 m	4.50 m	4.49 m
Trim (bow=+)	-0.16 m	- 0.26 m	-0.32 m	-0.31 m
List (PS=+)	+ 1.7 deg	+ 1.52 deg	+ 1.46 deg	+2.36 deg
GM0	1.52 m	1.48 m	1.45 m	1.44 m
Total weight	1802.6 t	1770.7 t	1752.7 t	1746.4 t

3.3. Engines, Generators and propulsion system

3.3.1. Propeller properties

The propeller of Aranda is a controllable pitch propeller with four blades. The propeller is ducted and has a rudder behind. The ducted propeller increases the thrust at lower speeds.



Figure 17: Propeller and rudder of Aranda

The propeller is a controllable pitch propeller (CP). The forward and backward speed is adjusted by changing the pitch position of the blades. The position of the blades is stated as percentage of the maximum pitch for forward speed.

Propeller data:

Diameter (form blade tip to blade tip): 2.6m
Hub diameter: 0.81m

Since the ice resistance is determined in dependency on the open water performance, the propeller diameter is the only information required according to the formulas.

3.3.2. Propulsion System

The propulsion system consists of two engines, two generators, one mechanical gearbox and one propeller shaft. The engines and the propeller shaft are running on constant rpm's and thus the power variation is achieved by varying the torque. The torque is again coupled to the propeller pitch.

The engine power is delivered in dependence on the propeller pitch, since the propeller pitch is the only parameter that is adjusted from the bridge in order to change the speed.

The engine loading is purely depending on the torque, which can be confirmed by looking at regular KT/KQ curves. Additionally it was observed that whenever ice hit the propeller blades (felt by vibration coming from the stern according to the captain) the

propeller pitch was increased automatically and the engine was overloaded. The rpm's have been kept constant at all times. This observation proves the above since ice hitting the propeller increases the drag on the propeller blades and therewith the torque on the shaft and requires a higher engine loading which often results in an engine overloading. This is a known problem of mechanical connections between the propeller shaft and engines for ice going.

3.3.3. Engine power and shaft power

Prefacing it must be known that the monitoring system of the engines is achieved via the fuel rack of the two engines. The fuel rack is a bar that indicates the position of the fuel rack and the therewith related fuel loading. The fuel rack position is linearly related to the power.

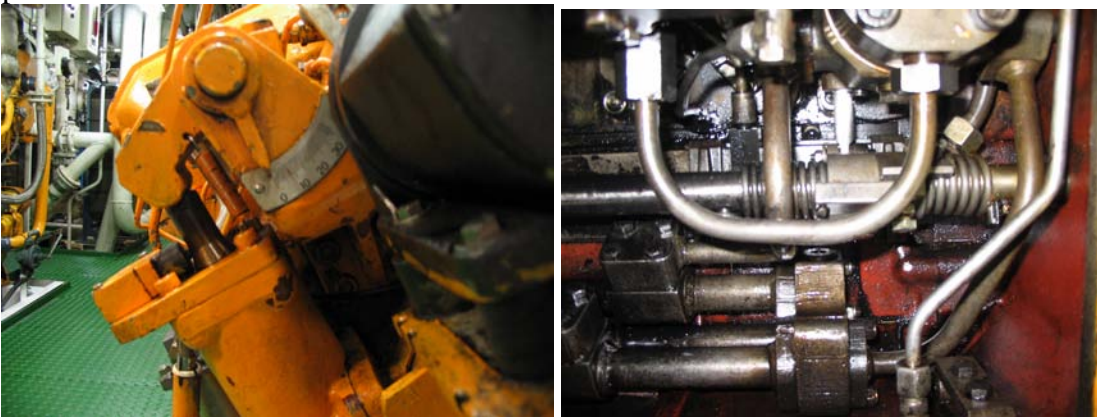


Figure 18: Fuel rack - indicator outside engine (left) and rack lever on the inside (right)

The position of the fuel rack is only set at zero in case the engine is switched off. When the engine is running on low power, without powering the propeller shaft the fuel racks are at 24% - 28% of maximum position. The generated power in this condition is purely transferred to power auxiliary systems such as lubing and cooling system.

The advantage of using the fuel rack as an indication system is that the fuel rack was installed that way that the fuel rack position has a linear dependency to the delivered power of the engine.

For feeding the ship systems with electric energy, generators are connected to both engines and the power of the generators has to be subtracted from the power delivered to the propeller shaft.

3.4. Engines and Generators

3.4.1. Main engine # 1

For the power assessment, the data from the original engine test documents have been used. The measured data from the initial installation have been taken to interpolate the engine power for 980 rpm in dependence on the position of the fuel rack. The engine is running constantly with the same rpm, which naturally varies a bit.

In the following text it is explained how the power and fuel rack properties are determined.

The data obtained from the original test tables are listed in table 3.

Table 3: Engine 1 powering data

power [kW]	fuel rack position [mm]	power in %	rpm
1700	27,5000	100,00%	1000
1275	22,5000	75,00%	1000
1275	23,0000	75,00%	908
850	18,5000	50,00%	794
850	17,5000	50,00%	1000

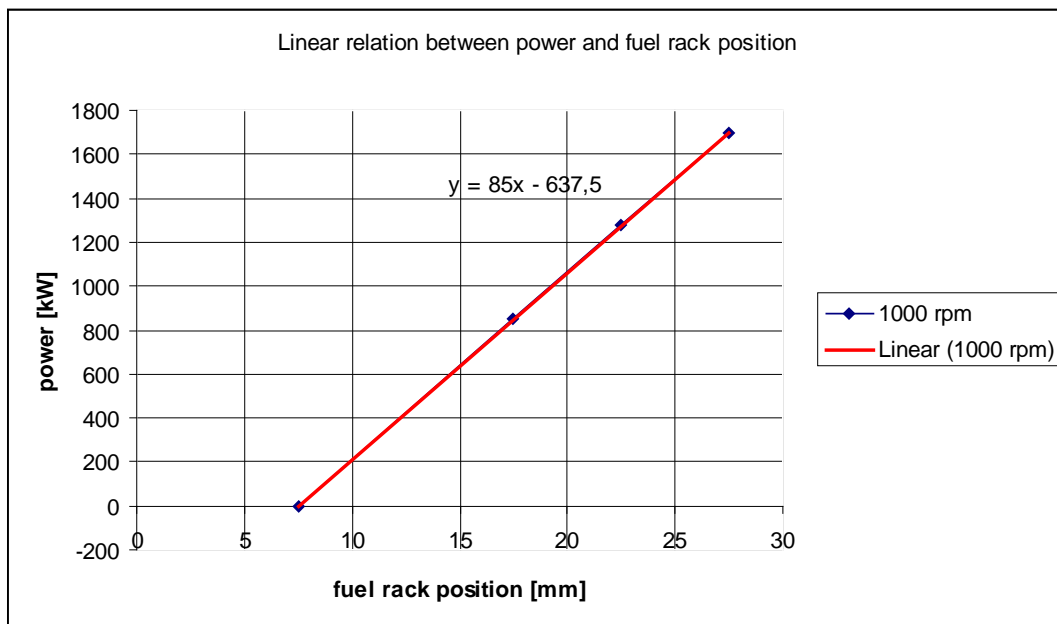


Figure 19: Fuel rack position versus delivered power at 1000 rpm

Figure 19 above shows three measured power values for 1000 rpm and the linear regression further proves that at 27% fuel rack position, respectively 7.5 mm the power delivery to the propeller shaft is zero (that is the power requested by the auxiliary systems).

The finding from above allows the conclusion that the relation between the fuel rack position and the rpm is linear, because the rpm's are related linearly to the power by the torque. That allows plotting the rpm's versus the fuel rack position for one particular power-level.

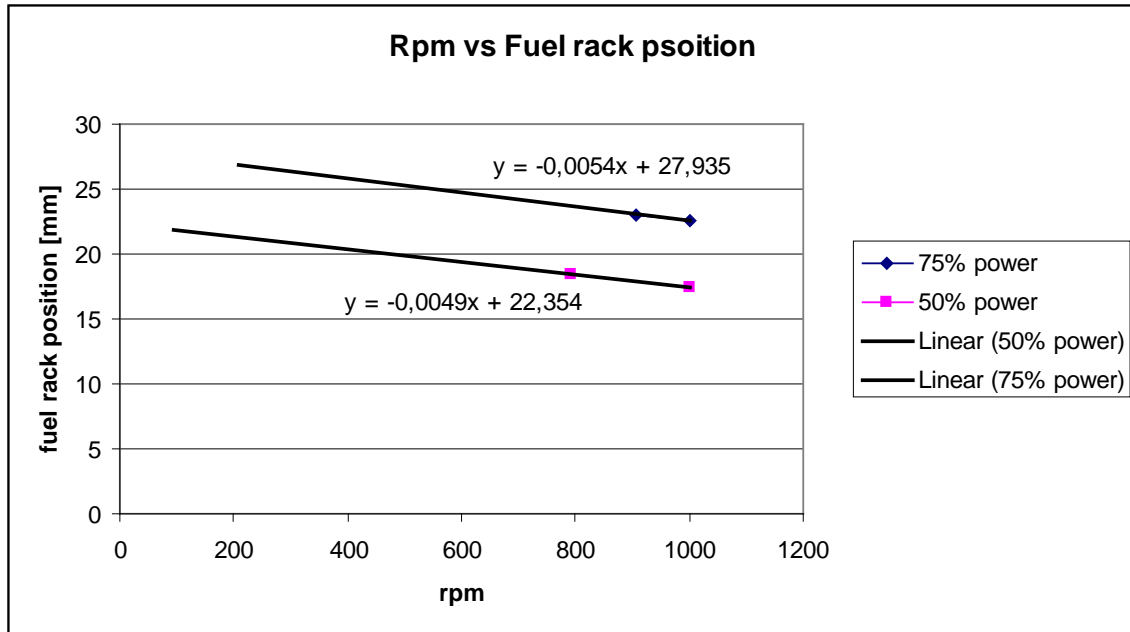


Figure 20: fuel rack position versus rpm for engine #1

The plot above including the equations of the linear regressions enables determining the fuel rack position for both power outputs (75% and 50%) at 980 rpm (or at any other rpm), which in turn delivers data for a new linear inter- and extrapolation of the power output and the fuel rack position for 980 rpm.

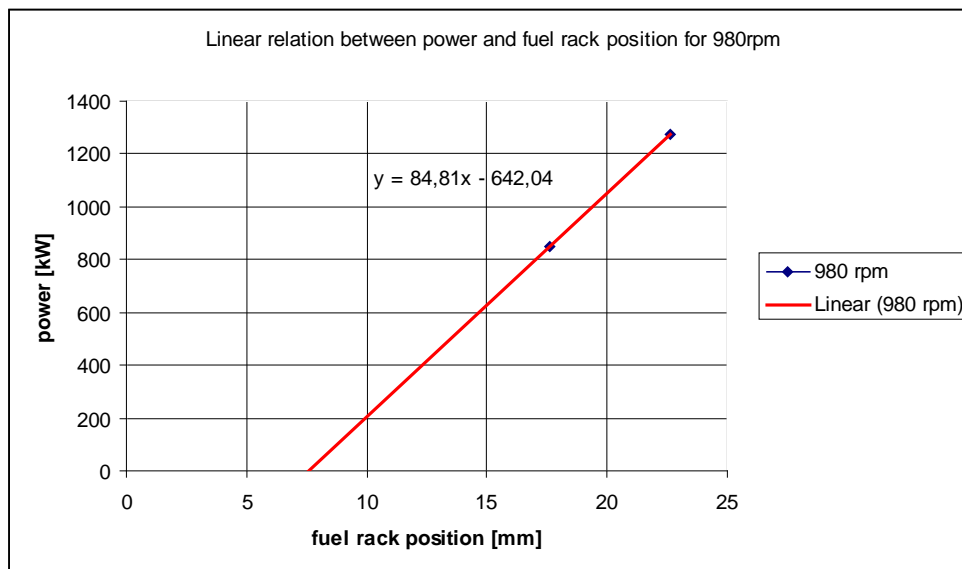


Figure 21: Power - fuel rack position relation for 980 rpm of engine 1

3.4.2. Main engine # 2

Main engine 2 has the following properties

Table 4: Engine 2 powering data

power [kW]	fuel rack		rpm
	position [mm]	power in %	
1300	31	1	1000
975	25	0,75	1000
975	26	0,75	908
650	21	0,5	794
650	19,5	0,5	1000

The measured data from the initial installation have been taken to interpolate the engine power for 950rpm in dependence on the position of the fuel rack. The number of revolution varies naturally a bit, but stays mainly constant. The procedure for determining the power is found in 3.4.1 and thus below only the final plot for 950rpm of engine #2 is stated.

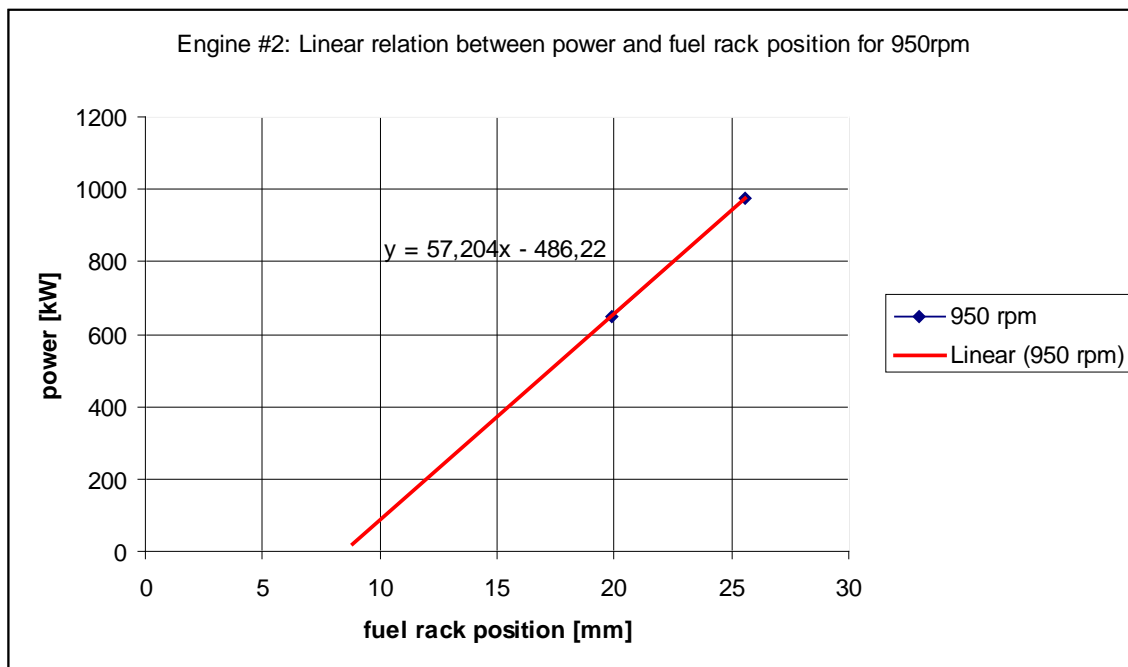


Figure 22: Power - fuel rack position relation for 950 rpm of engine 2

3.5. Propeller shaft power

Knowing the power on the propeller shaft is essential to assess the resistance in ice. The APIS monitoring system monitors the fuel rack position, the power of the generators, the rpm's of the engines and the rpm of the propeller shaft.

Determining the engine power of both engines according to the fuel rack position enables calculating the torque on the shaft leading to the gearbox which is attached to the propeller shaft. Knowing the rpm's of both engine shafts and of the propeller shaft, the gear ratio can be determined and there from the torque on the propeller shaft, respectively the shaft power.

The torque on the propeller shaft is further depending on the mechanical losses in the mechanical systems between the engines and the propeller screw. The overall efficiency is depending on the single efficiencies of the mechanical systems.

Assumed efficiencies:

Table 5: Propulsion system efficiencies

Efficiency	Value
Efficiency of the E-Generators on engine shaft	92%
Gearbox efficiency	95%
Efficiency due to shaft torsion	99%
Shaft bearings efficiency	99%
Bearing sealing and lubing efficiency	99%

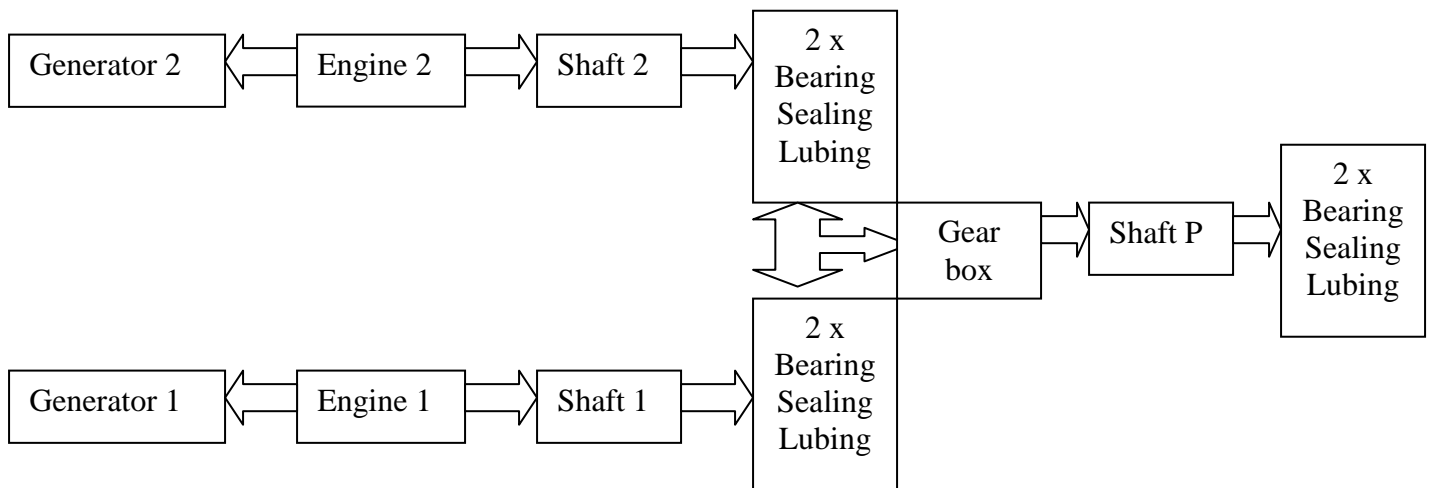


Figure 23: Propulsion System

Table 6: Symbols used in Figure 23

Item	Abbreviation
Generator power	GP
Generator efficiency	e_GP
Engine power	EP
Gearbox power from engine #x	GB_x
Gear box efficiency	e_GBP
Shaft torsion efficiency	e_ST
Lubing, bearing, sealing efficiency	e_B
Power at screw	PS

Related to Figure 23 the calculation of the available power (PS) on the propeller screw is determined according to equation

$$GB_x = (EP - \frac{100\%}{e_{GP}} GB) * e_{ST} * e_B^2 \quad (3)$$

$$PS = (GB_1 + GB_2) * e_{GBP} * e_{ST} * e_B^2$$

4. Cruise data and map

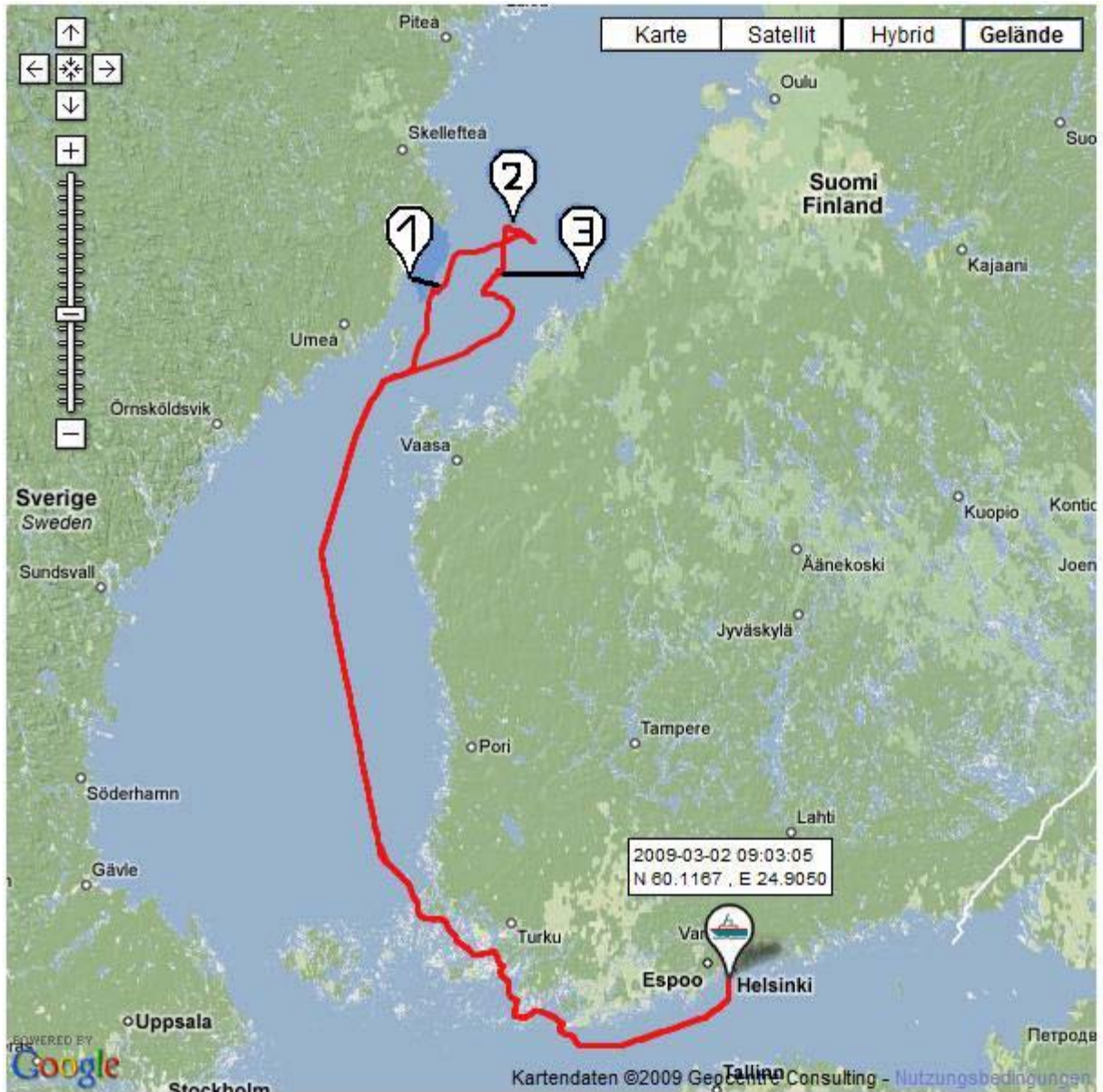


Figure 24: Station during Aranda ice cruise (FMI website)

The three marks in Figure 24 represent the three ice stations BOB 1, BOB 2 and BOB 3.

5. Open Water Performance

The open water performance was assessed by varying the propeller pitch in open water. The open water test was done twice. Once on the way from Helsinki to the Bay of Bothnia and once on the way back. On the way to the bay of Bothnia the ship encountered many waves. On the way back the sea was in very calm state, after leaving the ice covered areas. The open water performance was assessed in the IM (ice mode), which means that both engines are connected to the propeller shaft. Documents of the open water performance have been found as well, but it is not stated in what mode the propeller shaft was driven.

In open water the obtained data for the vessel speed and the power on the propeller shaft have been used to determine the net-thrust curve (Kujala and Sundell, 1992).

$$T_{pull} = K_e (D_p P_{sh})^{\frac{2}{3}} \quad (3)$$

$$T_{net} = T_{pull} \left(1 - \frac{1}{3} \frac{v}{v_{max}} - \frac{2}{3} \left(\frac{v}{v_{max}} \right)^2 \right) \quad (4)$$

The used parameters are

v:	actual ship speed
vmax:	maximum speed
Tpull:	bollard pull
Ke:	factor including the number of propellers, which is 0.78 for single screw propulsion as Aranda.
Dp:	propeller diameter
Psh:	total shaft power

The speed variation on Aranda is set by varying the propeller pitch. The net-thrust curves for dedicated pitch positions of Aranda, according to equation (5), are seen in Figure 25.

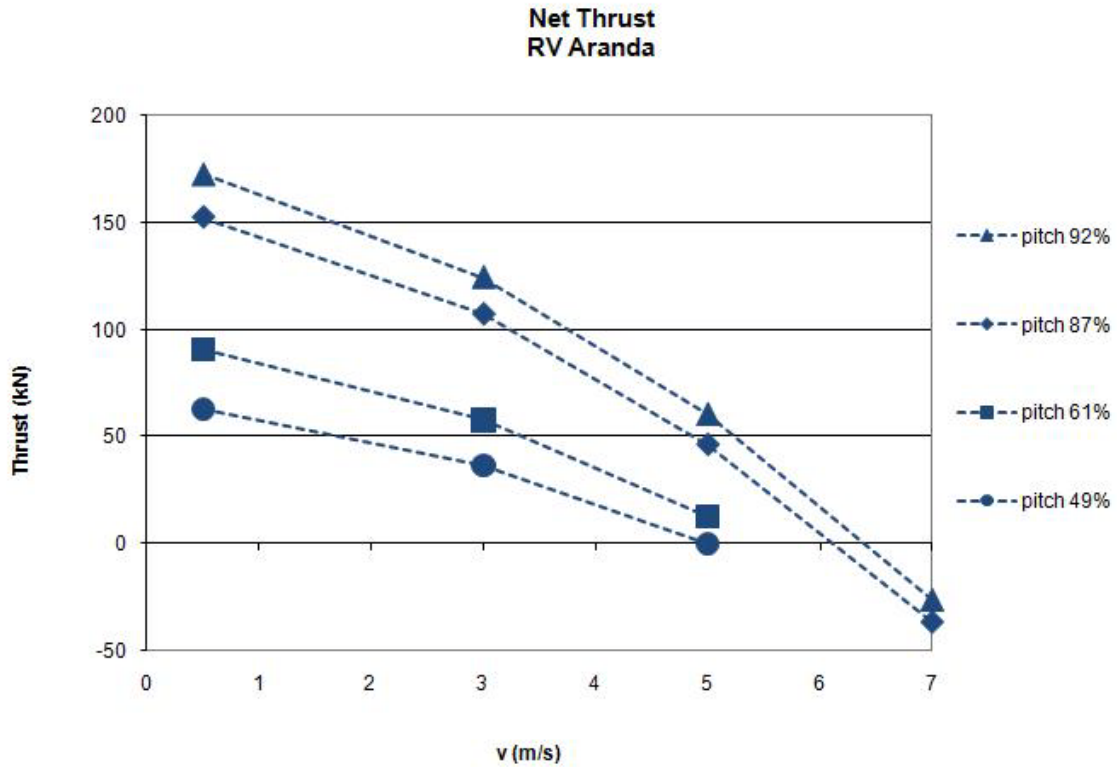


Figure 25 Theoretical Net Thrust Curve

6. Performance in ice

6.1. Theoretical performance in ice

The performance in ice is related to the performance in open water. The operational limits in level ice are determined by the intersections between the net-thrust curves and the theoretical determined ice resistance for various ice thicknesses.

Ice Resistance vs Speed

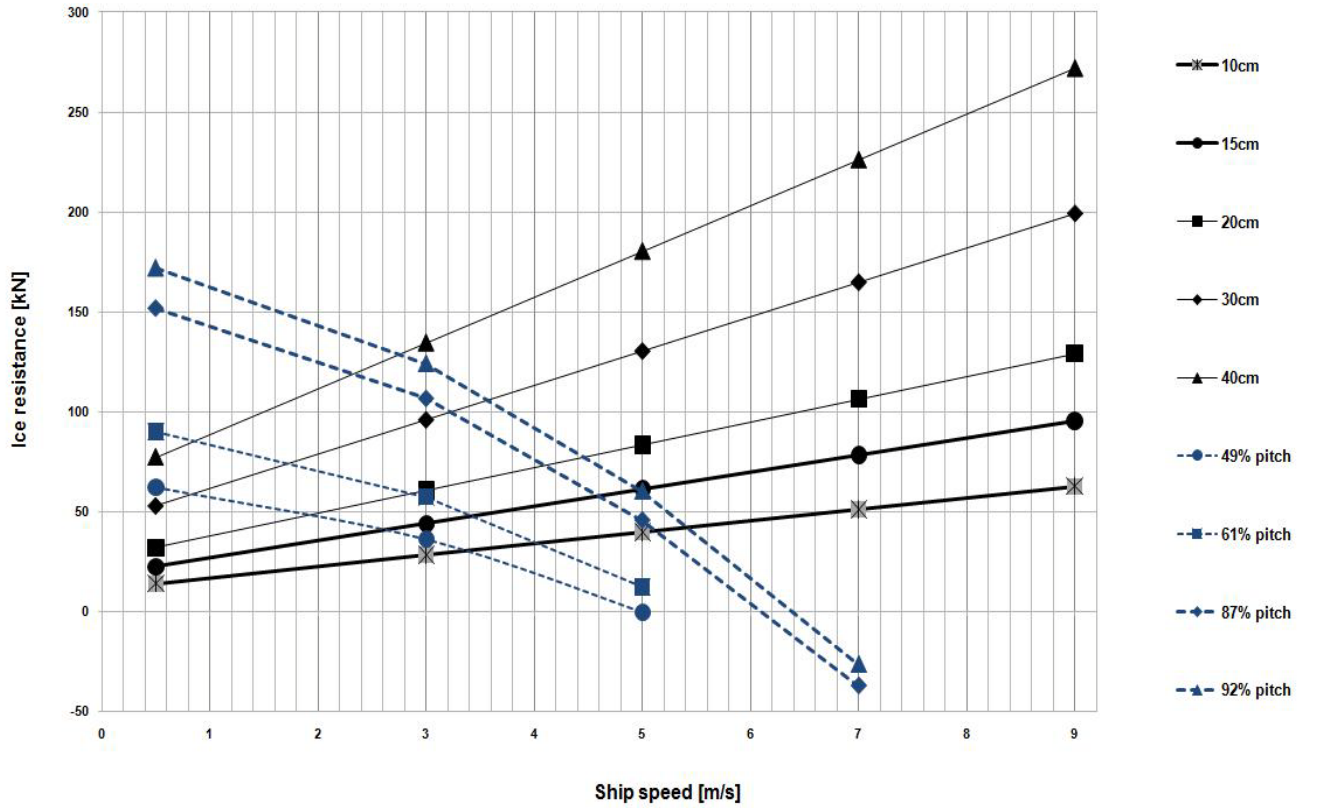


Figure 26: Aranda's ice resistance (straight lines according to particular ice thickness) versus net thrust in dependence on the pitch position of the propeller blades in %

The ice resistance in level ice is determined according to an empirical formula developed by K. Riska et al [5], which is based on the findings Ionov (1988) and Lindqvist (1989). The ice resistance is linear dependent on the ship speed.

$$R_i = C_1 + C_2 v$$

$$C_1 = f_1 \frac{1}{2 \frac{T}{B} + 1} BL_{par} h_i + (1 + 0.021\phi)(f_2 B h_i^2 + f_3 L_{bow} h_i^2 + f_4 BL_{bow} h_i) \quad (5)$$

$$C_2 = (1 + 0.063\phi)(g_1 h_i^{1.5} + g_2 B h_i) + g_3 h_i (1 + 1.2 \frac{T}{B}) \frac{B^2}{\sqrt{L}}$$

The constants used in equation

$$R_i = C_1 + C_2 v$$

$$C_1 = f_1 \frac{1}{2 \frac{T}{B} + 1} BL_{par} h_i + (1 + 0.021\phi)(f_2 B h_i^2 + f_3 L_{bow} h_i^2 + f_4 BL_{bow} h_i) \quad (6) \text{ are}$$

$$C_2 = (1 + 0.063\phi)(g_1 h_i^{1.5} + g_2 B h_i) + g_3 h_i (1 + 1.2 \frac{T}{B}) \frac{B^2}{\sqrt{L}}$$

found in Table 7: Constants for ice resistance.

Table 7: Constants for ice resistance

$$f_1 = 0.23 \frac{kN}{m^3}$$

$$f_2 = 4.58 \frac{kN}{m^3}$$

$$f_3 = 1.47 \frac{kN}{m^3}$$

$$f_4 = 0.29 \frac{kN}{m^3}$$

$$g_1 = 18.9 \frac{kN}{\left(\frac{m}{s \times m^{1.5}} \right)}$$

$$g_2 = 0.67 \frac{kN}{\left(\frac{m}{s \times m^2} \right)}$$

$$g_3 = 1.55 \frac{kN}{\left(\frac{m}{s \times m^{2.5}} \right)}$$

Figure 25 and Figure 26 represent the available net-thrust and finally the intersection between the net-thrust curve and the resistance curve represent the limiting speed in the particular ice thickness (Figure 27).

The intersections between the resistance curve and the net thrust curve reflect the limiting ice thickness for a particular propeller pitch position. The intersections of the curves above represent the so called h-v curve which reflects for which particular ice thickness and speed the particular propeller pitch reaches its limit.

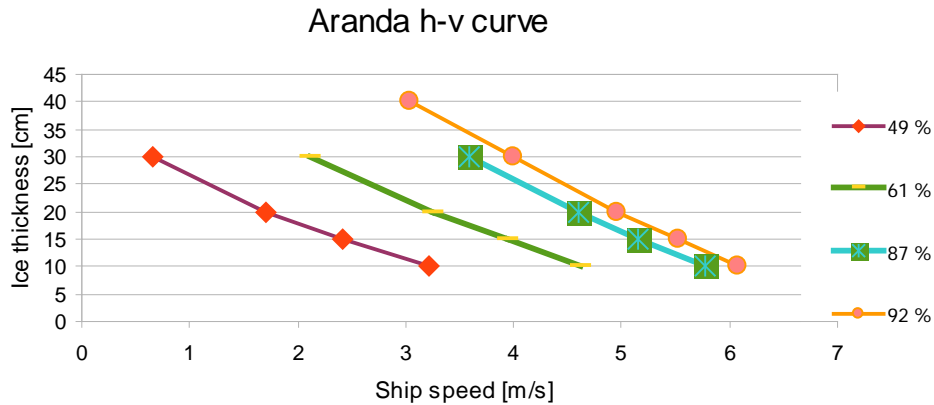


Figure 27 Aranda h-v curve

The h-v curve is plot for the four different pitch positions stated in percentages of the full pitch (100%). The h-v curve is valid for level ice only.

6.2. Practical performance in ice

6.2.1. Measurements

The required data for validating the h-v diagram were the ship speed and the ice thickness. The ship speed was taken from the on-board system and the ice thickness was appraised visually from the bridge. The full-scale measurements have been reduced to a small number since only those data were taken into account where it was very sure that the ship was sailing in level ice and not hitting any ridges, leads or other.

In order to verify the theoretical results from the previous section, the speed and the ice thickness have been monitored while sailing in ice. The ship speed has been recorded by the on board GPS of the ship and the ice thickness has been determined visually from the bridge. The estimation of the ice thickness was supported by the experienced captain and reference thickness measurements at the ice stations. However the estimation of the thickness is still coarse and thus it is assumed that the ice thickness can be determined with accuracy of +/- 5cm.

Limiting ice thickness depending on propeller pitch 94% - Aranda, 7.3.2009

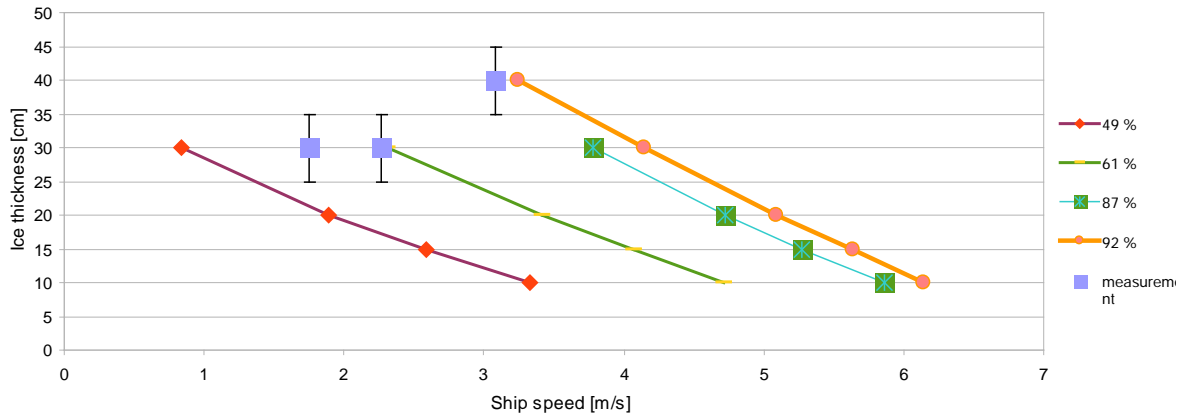


Figure 28: Measurements at 94% pitch

Limiting ice thickness depending on propeller pitch 89% - Aranda, 11.3.2009

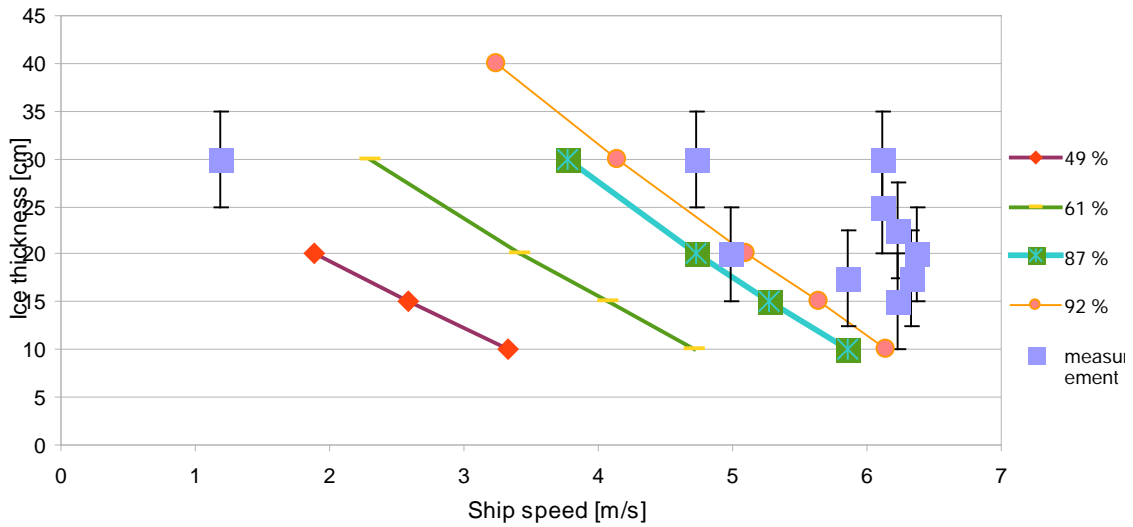


Figure 29: Measurements at 89% pitch position

Limiting ice thickness depending on propeller pitch 78% - Aranda,
11.3.2009

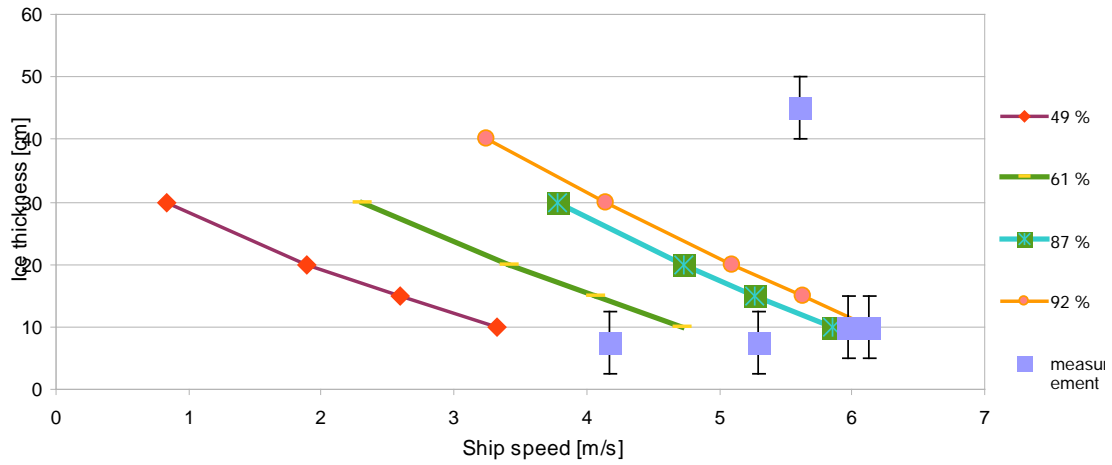


Figure 30: Measurement at 78% pitch position

Limiting ice thickness depending on propeller pitch 92% - Aranda,
11.3.2009

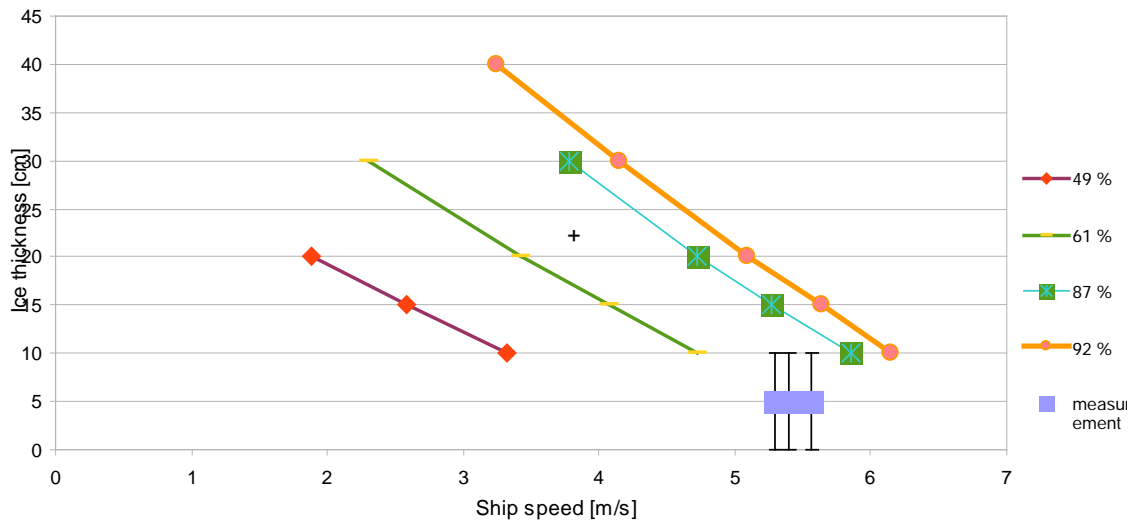


Figure 31: Measurement at 92% pitch position

Limiting ice thickness depending on propeller pitch 89% - Aranda,
7.3.2009

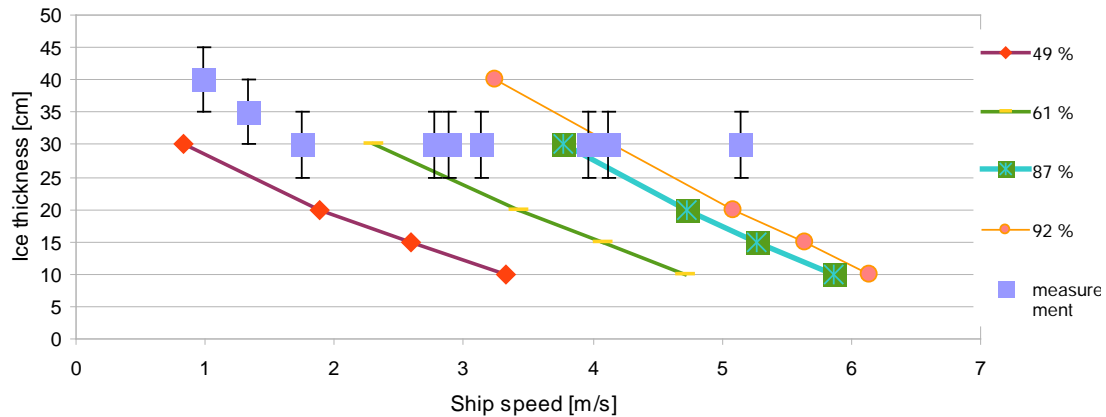


Figure 32: Measurement at 89% pitch position

6.2.2. Evaluation of the measurements

The plots from Section 6.2.1 show that the theoretically predicted h-v curve matches with some values but not with all of them. One major reason for that lies in the randomness of the ice properties and that sometimes floes might have been encountered instead of level ice or that some ice thickness variations occurred that could not be assessed visually from the bridge. The measurements of the mechanical properties seen in Figure 14, Figure 29 and Figure 32 reflect the variation of the ice properties within the bay of Bothnia very well. Figure 29 and Figure 32 refer to the same pitch position, but completely different full-scale measurements are obtained.

6.3. Accuracy of the assessment of the performance in ice

The accuracy of the assessment is depending on the accuracy of the used parameters. The determination of the theoretical performance in ice is depending on many factors, which accuracy or offset can not be determined such as the main dimensions, fuel rack position and its recording. Due to so many uncertainties it was decided not to subject the resistance and the thrust to a systematic error analysis. The systematic error analysis is going to be incorporated in the data of the measured performance in terms of the ice thickness, only.

Since the ice thickness was determined visually the possible error has to be considered being at +/- 5cm.

The speed data that are used are those given by the ship onboard systems, which are already filtered.

7. Summary

According to the figures in Section 6.2.1 it is seen that some measured values meet the predetermined h-v curve, but not all of them. The measurements of the ice properties show that the ice properties are subjected to many parameters and parameters such as salinity and temperature varied over a relatively wide band, which are considered having a significant impact on the mechanical ice properties and thus on the resistance.

In order to make a more accurate prediction it would have been necessary to carry out thickness and strength measurements along a 2km long track which is then sailed by the ship. That was however not possible since the ship was mainly surrounded by drift fields and the direction of the location departure could never be determined in advance. The enormous amount of drift ice also raises the uncertainty of the pure level ice occurrences.

8. Conclusions

It has been observed that some measured values are meeting the theoretical predicted h-v curve, but the amount of obtained data is too little to draw a final conclusion on that. Thus it would be necessary to carry out even more measurements of h-v data on board of ships sailing in level ice. It is further necessary to carry out these tests on different types of ships, since it was observed that the performance of the Aranda was subjected to significant variations at lower speeds which may lead to the conclusion that especially smaller ships are not suitable for appraising the thickness in thicker ice or at lower speeds, because the non-homogeneity of the ice and the randomness and variation of some properties might affect the performance significantly. It requires however more empirical tests with different ships of different sizes to prove this theory. Since the ice properties are not affecting the theoretical thrust curve directly, since empirical factors are incorporated that represent standard strength values, it would not even be necessary to measure ice properties in the first place, but only to monitor speed and ice thickness.

References

- [1] Kujala, P. and Sundell, T. (1992) – Performance of ice strengthened ships in the northern Baltic Sea in winter 1991, Report M-117, Otaniemi, ISBN 951-22-0917-9
- [2] ITTC – Recommended procedures and guidelines, Testing and Extrapolation Methods Ice Testing Test Methods for Model Ice Properties, 2002
- [3] Varsta, P. (1983) – On the mechanics of ice load on ships in level ice in the Baltic sea, Dr. thesis, ISBN 951-38-1843-8
- [4] Kujala, P. – On the statistics of ice loads on ship hull in the Baltic (1994), DSC thesis, Report M-116, ISBN 951-666-432-6
- [5] Riska, K. et al. (1998) Performance of merchant vessels in the Baltic, Winter Navigation Research Board – Research Report No 52, Finnish Maritime Administration, ISBN 951-49-0880-5
- [6] Schulson, E. and Duval, P. (2009) – Creep and Fracture of Ice, Cambridge University Press, ISBN 978-0-521-80620-6
- [7] Cammaert, A. and Muggerridge, D. (1988) – Ice interaction with offshore structures, Van Nostrand Reinhold Co. Inc., ISBN 978-0442216528

Aalto University, School of Science and Technology. Faculty of Engineering and Architecture. Department of Applied Mechanics. Series AM

- TKK-AM-14 Kim Salmi
TARGETING ACCIDENT PRONE SHIPS BY THEIR BEHAVIOUR AND SAFETY CULTURE
- TKK-AM-13 Pentti Kujala; Kaj Riska
TALVIMERENKULKU
- TKK-AM-12 Janne Ranta
SIMULATION OF ICE RUBBLE FAILURE AGAINST A CONICAL STRUCTURE WITH ARBITRARY LAGRANGIAN-EULERIAN ELEMENT METHOD
- TKK-AM-11 Heini Kiuru; Kim Salmi
ACCIDENT ANALYSIS; THE TOOL FOR RISK EVALUTION
- TKK-AM-10 Arsham Mazaheri
PROBABILISTIC MODELING OF SHIP GROUNDING; LITERATURE REVIEW
- TKK-AM-9 Risto Jalonen; Kim Salmi
SAFETY PERFORMANCE INDICATORS FOR MARITIME SAFETY MANAGEMENT; LITERATURE REVIEW
- TKK-AM-8 Tommi Mikkola
SIMULATION OF FORCES ON SHIP-LIKE CROSS-SECTIONS IN BEAM WAVES
- TKK-AM-7 Sören Ehlers
A THIN SPHERICAL PLATE UNDER HEMI-SPHERICAL PUNCH
An experimental study of a plate subjected to a displacement controlled punch
- TKK-AM-6 Jutta Ylitalo; Maria Hänninen; Pentti Kujala
ACCIDENT PROBABILITIES IN SELECTED AREAS OF THE GULF OF FINLAND
- TKK-AM-5 Sankar Arughadhoss
FLOW SIMULATION OF BOX COOLER
An Experimental Study of Buoyant Water Flow in a Box Cooler

ISBN 978-952-60-3160-6 (PDF)
ISSN 1797-6111 (PDF)